Magazine of Concrete Research
Volume 68 Issue 13

Time-dependent brittle creep-relaxation failure in concrete
Wang, Zhang and Hao

Magazine of Concrete Research, 2016, **68**(13), 692–700
http://dx.doi.org/10.1680/jmacr.15.00186
Paper 1500186
Received 03/05/2015; revised 12/12/2015; accepted 21/12/2015
Published online ahead of print 11/02/2016
Keywords: creep/failure/stress

ice
Institution of Civil Engineers
publishing

Time-dependent brittle creep-relaxation failure in concrete

Ying-chong Wang
MSc student, School of Civil Engineering and Mechanics, Yanshan University, Qinhuangda, People's Republic of China

Bao-Ju Zhang
MSc student, School of Civil Engineering and Mechanics, Yanshan University, Qinhuangda, People's Republic of China

Sheng-Wang Hao
Professor, School of Civil Engineering and Mechanics, Yanshan University, Qinhuangda, People's Republic of China; The State Key Laboratory of Non-linear Mechanics, Institute of Mechanics, Chinese Academy of Science, Beijing, People's Republic of China
(corresponding author: haoshengwang@gmail.com)

In real-world engineering applications, concrete is usually subjected to both creep and stress relaxation. Observations are necessary to understand this coupling process. This paper presents the results of brittle creep-relaxation experiments performed on concrete. Instead of tending to an asymptotic value, the stress in all the test specimens dropped sharply with a rapid increase in the strain before failure, when the boundary displacement was kept constant. The acceleration in the tertiary stage exhibited power-law behaviour, with the exponent $-\alpha$ being $-0{\cdot}58 \pm 0{\cdot}13$ for the stress rate and $-0{\cdot}56 \pm 0{\cdot}12$ for the strain rate. For each specimen, the time-to-failure exhibited power-law dependence on the secondary creep (relaxation) rate, with the exponent being $0{\cdot}97 \pm 0{\cdot}09$ for strain and $0{\cdot}98 \pm 0{\cdot}09$ for stress. These results suggest that it should be possible to predict the time-to-failure of concrete by monitoring its behaviour during the steady and critical stages.

Notation

A, B	constants
$\mathrm{d}\varepsilon/\mathrm{d}t$	strain rate
$\mathrm{d}\sigma/\mathrm{d}t$	stress rate
$\mathrm{d}\sigma/\mathrm{d}U$	first-order derivative of stress with respect to displacement
F	force
f	failure
t	time
t_f	failure time
t_0	start time of creep-relaxation phase
t_1, t_2, t_3	times corresponding to three successive points
U	displacement of crosshead of testing machine
u	deformation of concrete sample
u_f	failure deformation of concrete sample
u_m	deformation of loading apparatus
v	rate of an observable quantity, such as strain or stress
v_1, v_2, v_3	rates at three successive points
α	critical exponent
ε	strain
λ_s	slope of secondary segment
$\lambda_{\mathrm{s}\varepsilon}$	slope of secondary segment for strain
$\lambda_{\mathrm{s}\sigma}$	slope of secondary segment for stress
σ	stress
σ_max	maximum stress

Introduction

The time dependence of the fracture behaviour of concrete materials and the damage they undergo is of great interest (Aslani and Maia, 2013; Barpi and Valente, 2005; Bazant and Xiang, 1997; Bocca and Antonaci, 2005; Brooks, 2005; Carpinteri *et al.*, 1997; Geng *et al.*, 2012). For instance, being able to predict the time-dependent failure of concrete is essential for understanding many aspects of concrete engineering, including the ability to predict and design the behaviour of concrete structures. Creep and stress-relaxation tests are the two essential methods used to assess the time-dependent behaviour of materials. Creep is the time-dependent deformation of a material subjected to a constant stress, and can lead to the failure of the material over time. In contrast, stress relaxation describes how materials under constant deformation relieve stress.

The phenomena of creep and stress relaxation have been recognised as being critical with respect to concrete by both structural and material engineers. Many mechanisms considered to be responsible for the time-dependent behaviour of concrete or having an effect on it have been proposed and studied (Bazant, 2001; Hamed, 2015; Rossi *et al.*, 2012). These have enabled researchers to formulate mathematical theories (Bazant, 2001, Bazant and Baweja, 1995; Choi *et al.*, 2015) to describe the time-dependent behaviour of concrete under load. However, despite major successes, the phenomenon of creep is still far

from being fully understood (Bazant, 2001). Most of the previous studies on the creep behaviour of concrete have been performed at low stresses (Blechman, 2014; Brooks and Neville, 1977; Forth, 2015; Ranaivomanana *et al.*, 2013). In contrast, the brittle time-dependent behaviour of concrete under high and sustained stresses is not well known.

As a typical quasibrittle material, concrete degrades because of the initiation and propagation of microcracks. Crack evolution is a key factor resulting in the delayed failure of concrete (Rossi *et al.*, 2014). It is widely accepted that viscoelasticity and crack growth govern the long-term deformability of concrete, and thus its service behaviour and durability (Denarié *et al.*, 2006). For low load levels, the viscoelastic behaviour of concrete is quasilinear, and crack growth is usually absent (Blechman, 2014). On the other hand, for high load levels, the cracks grow and interact with the viscoelasticity. In order to address this issue, researchers have been studying the interaction between crack propagation and the time-dependent behaviour of concrete (Denarié *et al.*, 2006; Omar *et al.*, 2009; Saliba *et al.*, 2013).

The relationship that exists between creep and stress relaxation in the case of concrete has been the focus of previous studies (Klug and Wittmann, 1970). Efforts have also been made to evaluate the stress-relaxation parameters (Gao *et al.*, 2013). However, it is worth noting that, in the case of actual engineering projects, concrete is usually subjected to both creep and stress relaxation. Thus, elucidating the mechanism by which these two phenomena combine and result in the failure of concrete is the key to evaluating the long-term performance of concrete structures and the time-dependent behaviour of concrete. Further, understanding this combining process is particularly important for the design and safety assessment of concrete engineering structures.

In this paper, the investigated concrete material and the experimental techniques used are described first. Then, the results of static monotonic loading tests performed to determine the load levels for the creep-relaxation tests are presented. Next, the results of uniaxial compressive creep-relaxation tests, which were performed on the concrete specimens in order to observe their failure behaviours, are described. The stress and strain curves for the specimens subjected to failure and their critical behaviours are analysed. The lifetime of concrete is found to be dependent on the secondary stage.

Material and specimen preparation

The concrete specimens used were rectangular blocks (160 mm high and 40×40 mm in cross-section) and were cast using an accurately machined steel mould. The composition of the concrete mixture used was as follows: silicate cement: 320 kg/m^3; water: 185 kg/m^3; fine aggregate (natural river sand; fineness modulus of 2·41): 757 kg/m^3; limestone coarse aggregate (4·75–16 mm in size; ratio of particles 9·5–16 mm in size to 4·75–9·5 mm in size = 7:3): 1135 kg/m^3; and water-reducing admixture (naphthalene-based superplasticiser): 2·2 kg/m^3. The specimens were cured for 28 d in a fog room at a temperature of 20 ± 2°C and relative humidity of more than 95%.

Experimental methods

The concrete specimens were uniaxially compressed in the vertical direction (160 mm) at room temperature using a screw-driven crosshead; a universal electromechanical testing machine equipped with a force sensor was employed for the purpose, and an offset load of 1 kN was used. The deformation, u, of the test specimen was measured using extensometers with a resolution of 1 μm located on the sides of the specimen.

Figure 1 shows the complete results for the creep-relaxation experiments performed on a typical specimen. The testing machine used real-time displacement control, and all the specimens were rapidly loaded to the initial deformation state (part OA in Figure 1(a)) before the creep-relaxation test. This involved limiting the ultimate crosshead displacement of the apparatus to $\sim 1{\cdot}1$ mm and the crosshead speed to 1·5 mm/min. The crosshead was then held at this position (part AB in Figure 1(a)), and the displacement of the test specimen was measured as it relaxed. As shown, the displacement was held constant after the crosshead had reached the initial position (Figure 1(a)); at this point, stress relaxation accompanied the increase in the deformation of the specimen (Figures 1(b) and 1(c)). Thus, the concrete specimens underwent a stress relaxation–creep coupling process. This coupling process induced further damage in the test specimens, eventually resulting in their sudden and brittle failure.

The time at which the test specimen failed macroscopically is defined as t_f. Further, t_0 (see Figure 1) is defined as the time at which the phenomena of creep and stress relaxation begin to couple; it is also the onset time of the initial displacement. It is obvious that the displacement (U) of the crosshead of the testing machine is a sum of the deformation of the loading apparatus (u_m) and that of the deformed concrete sample (u). Thus, the loading apparatus accumulates substantial elastic energy during the initial displacement stage. As a result, the deformation of the specimen cannot remain constant during the holding process, because the loading apparatus undergoes elastic recovery.

Results and discussion

Tests involving quasistatic, monotonically increasing displacement

For the initial calibration process, 21 samples were used, which were compressed under a monotonic load; the crosshead displacement was set at 0·05 mm/min (at a strain rate of approximately $5{\cdot}2 \times 10^{-6}$ s^{-1}), and the samples were loaded to failure (i.e. there was no hold step). The sizes and shapes of the

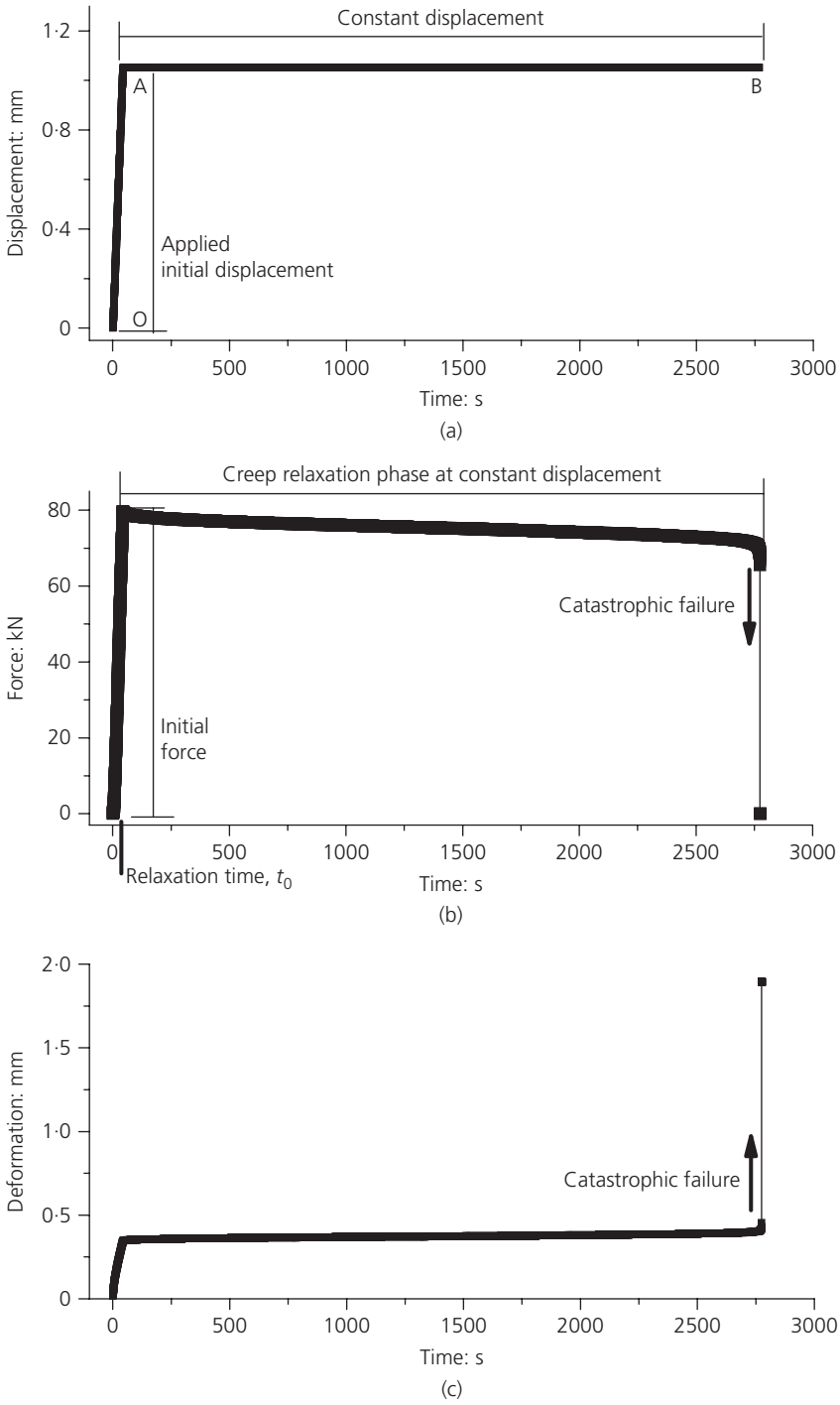

Figure 1. Example of the catastrophic failure observed in concrete during creep-relaxation tests. (a) Crosshead displacement plotted against time. The displacement remains constant once the specimen has been subjected to the initial displacement. (b) Force–time curve. The relaxation time, t_0, denotes the time corresponding to the peak force, which decreases thereafter with time. (c) Deformation of the tested specimen over time. The arrow denotes the direction of the jump in the force and the deformation associated with sudden catastrophic failure

specimens were the same as those used for the creep-relaxation tests. Figure 2 shows the displacement–stress curves for four of the concrete specimens.

The maximum stress ranged from 35·85 MPa to 51·39 MPa, with the mean peak stress being $42{\cdot}31 \pm 6{\cdot}44$ MPa (mean ± standard deviation). The displacement at the maximum stress

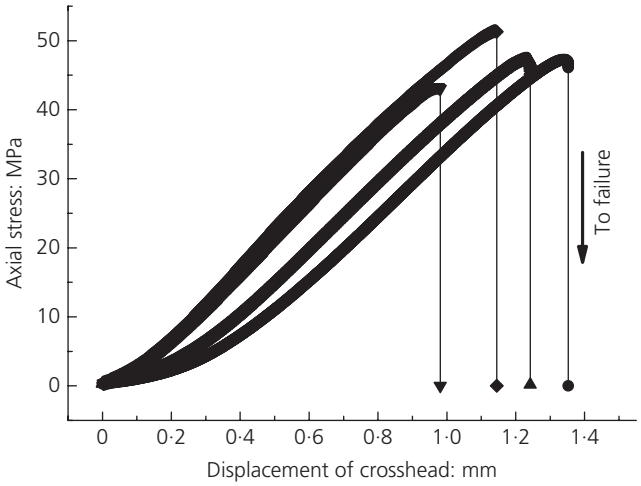

Figure 2. Dynamic rupturing induced in concrete under monotonic loading by keeping the displacement rate of the crosshead constant (0·05 mm/min). The specimen fails suddenly in the post-failure stage, once the peak force is reached. Some scatter exists in the peak forces and the failure displacements

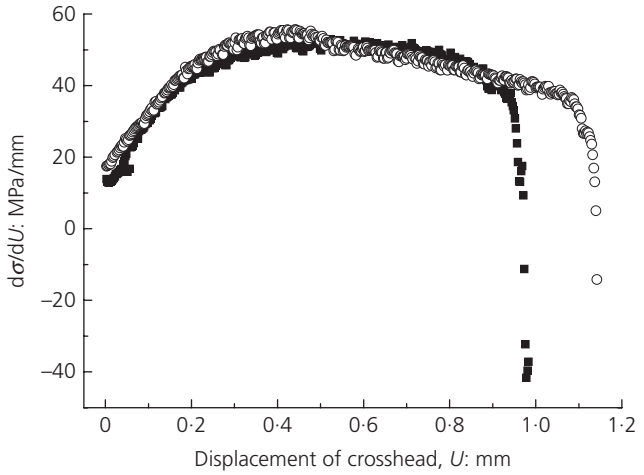

Figure 3. Plots of the relative changes in the stress with respect to the displacement ($d\sigma/dU$) for two of the concrete specimens

ranged from 0·97 mm to 1·34 mm, with the mean value being $1{\cdot}22 \pm 0{\cdot}17$ mm. Further, the corresponding deformation of the concrete specimens was $0{\cdot}65$ mm $\pm 0{\cdot}21$ mm. The failure displacement was $1{\cdot}25 \pm 0{\cdot}17$ mm, and the corresponding deformation, u_f, was $0{\cdot}75 \pm 0{\cdot}22$ mm.

In each case, the stress–displacement curves (see Figure 2) had the shape typical for concrete or rock deformed under compression. An initial hardening phase was followed by a pseudoelastic phase; this was followed by a roll-over to the peak stress. The peak stress was followed by a short phase of strain softening, which led to dynamic failure, as denoted by the drop in the stress.

In order to evaluate the changes in the stress with the increase in displacement, the curves for the first-order derivative of the stress with respect to the displacement ($d\sigma/dU$) were analysed for two of the concrete specimens (see Figure 3). It can be seen that, in the early stage of the compression test, the stress–displacement and stress–deformation curves were slightly convex in the upward direction. This hardening stage is either related to the elastic closing of the pre-existing cracks and pores or to the condition where the crack-closure rate exceeds the crack-opening and propagation rates. The curve then flattens; however, a peak can be seen in Figure 3. Beyond this peak, the rates of increase of the stress with respect to the displacement and deformation decrease. This is probably attributable to the crack-initiation, crack-opening and crack-propagation rates exceeding the crack-closure rate, and eventually leads to macroscopic failure. This transition point corresponds to the maximum in the curves. Therefore, it can be assumed that time-dependent brittle creep-relaxation failure occurs at a displacement greater than that corresponding to the transition point. In the present study, the displacements to which the specimens were subjected during the stress-relaxation–creep coupling tests were almost equal to the displacements corresponding to the maximum stress during the monotonic tests.

Brittle creep relaxation tests

Stress, strain level, initially applied displacement and energetic failure during brittle creep-relaxation tests

Figure 4 shows the curves for the axial stress and strain with respect to time for all ten samples for the creep-relaxation phase. It can be seen that all the specimens failed abruptly after being subjected to a constant displacement. The maximum stress was $50{\cdot}98 \pm 3{\cdot}16$ MPa (it ranged from 42·09 MPa to 54·79 MPa). Thus, the maximum stress during the creep-relaxation tests was slightly greater than the peak stress ($42{\cdot}31 \pm 6{\cdot}44$ MPa) during the monotonic loading tests. However, the deformation ($0{\cdot}38 \pm 0{\cdot}06$ mm) at the maximum stress was much smaller than that ($0{\cdot}65 \pm 0{\cdot}21$ mm) during the monotonic loading tests. It is clear that the loading apparatus stored much of the elastic energy during the initial loading stage. This stored elastic energy was released in the creep-relaxation phase and induced further deformations in the specimens, resulting in the observed drop in the stress.

A typical stress-relaxation process consists of the rapid initial relaxation of stress, which is followed by a slow relaxation stage, in which the stress decreases at a constant rate. In the present study, this decrease in the stress stopped abruptly because of the increase in the rate of stress loss and owing to deformations, which led to brittle failure. These results imply that, in heterogeneous brittle materials such as concrete, stress relaxation may induce catastrophic failure if the elastic energy

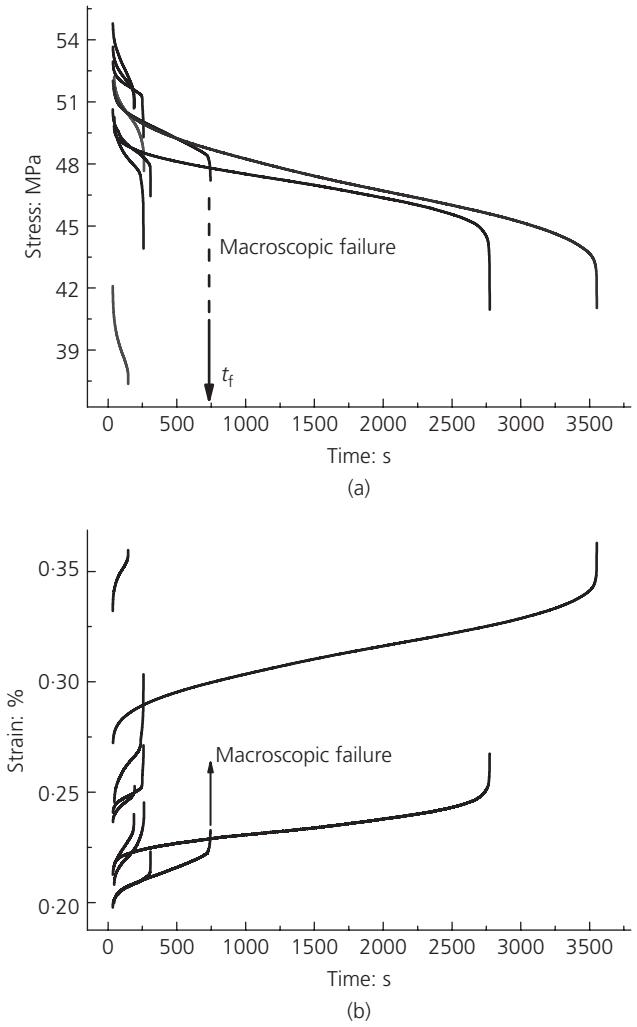

Figure 4. Experimental results corresponding to the stress relaxation–creep coupling process for the ten samples; the process induced catastrophic failure in all the specimens. The arrow indicates the time to failure, t_f, for one example. Temporal evolution of the (a) stress and (b) strain

stored in the surrounding environments can compensate for the fracture energy of the material.

In the case of a plastic material undergoing stress relaxation, the initial imposed elastic strain is replaced over time by an inelastic strain (Aifantis and Gerberich, 1975). As a result, the stress relaxes with time. However, for heterogeneous brittle materials such as concrete or rock, a drop in the stress is induced by the damage-relaxing stress. This delay in the occurrence of damage is associated with crack initiation and propagation. Further, the coalescence and growth of microcracks and microdefects lead to macroscale fractures.

Even in the case of a so-called stiff machine, localisation can result in catastrophic failure during creep relaxation. Localisation leads to a division of the material into a localised zone and other zones (Bazant and Pijaudier-Cabot, 1988; Hao *et al.*, 2010; Jansen and Shah, 1997; Shah *et al.*, 1994; Van Mier *et al.*, 1997). As soon as the elastic energy stored in these other zones becomes greater than the fracture energy of the localised zone, catastrophic failure will occur during creep relaxation.

Stages of brittle creep relaxation

As shown in Figures 1 and 4, during the creep-relaxation phase, in which the samples were subjected to a constant displacement, the concrete specimens exhibited an obvious creep relaxation behaviour. It was observed that the brittle macroscopic failure associated with the stress relaxation–creep coupling process followed a temporal sequence comprising three stages (see Figures 1(b) and 1(c) and Figure 4). In order to further characterise these three stages of the evolution of the creep-relaxation failure behaviour, the first derivatives of the stress and strain with respect to time (i.e. the rates of change of the stress and strain) were calculated; the curves for these are shown in Figure 5. As can be seen from Figures 4 and 5, after the crosshead of the test apparatus had been held at a constant displacement, all ten specimens exhibited a transient decrease in the stress and strain rates (Figure 4), in a manner similar to that seen during the so-called primary creep stage. This was followed by a steady-state creep-relaxation stage, during which the curves exhibited an approximately constant slope. The sequence ended with a rapid increase in the stress and strain and resulted in catastrophic failure.

There was a large variability in the failure time, t_f, values of the specimens (Figure 4) for almost similar displacements. The lifetime of a concrete specimen is strongly dependent on the magnitude of the applied external strain, the evolution of the damage behaviour of the concrete, and the ratio of the initial stiffnesses of the test machine and the specimen.

Scaling laws in the tertiary stage

Macroscopic scaling laws are necessary if one wishes to extrapolate the experimental results in order to understand the process of brittle creep relaxation in concrete at the time scales and strain rates corresponding to actual engineering applications.

The acceleration properties at the point close to failure can be used to make short-term predictions regarding the time to failure (Voight, 1989). A theoretical analysis (Hao *et al.*, 2012) has shown that the acceleration behaviour of the stress and strain rates near failure can be described in terms of power laws: $d\sigma/dt \approx A(1 - t/t_f)^{-\alpha}$ and $d\varepsilon/dt \approx B(1 - t/t_f)^{-\alpha}$, with $\alpha = 1/2$. In order to examine the critical behaviour of the power laws near failure, log–log plots of the axial stress and strain rates against $[1 - (t - t_0)/(t_f - t_0)]$ for the ten specimens were plotted; these are shown in Figure 6. As mentioned above, t_f represents the failure time and t_0 is the start time of the creep-relaxation

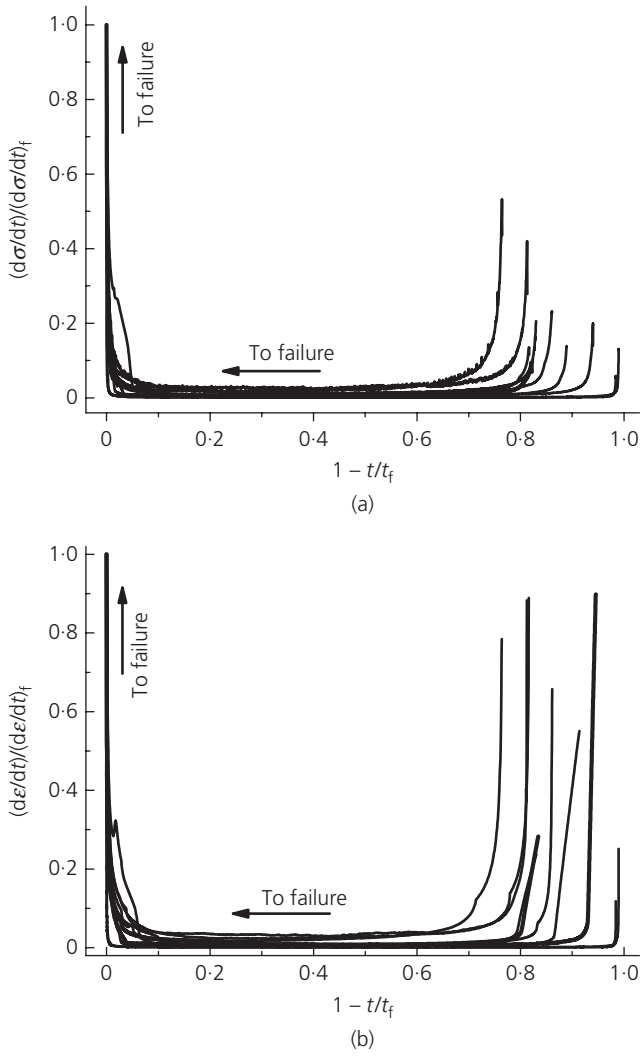

Figure 5. Axial stress and strain rates plotted against time for the ten concrete specimens corresponding to the creep-relaxation phase: (a) axial stress rate against time and (b) axial strain rate against time

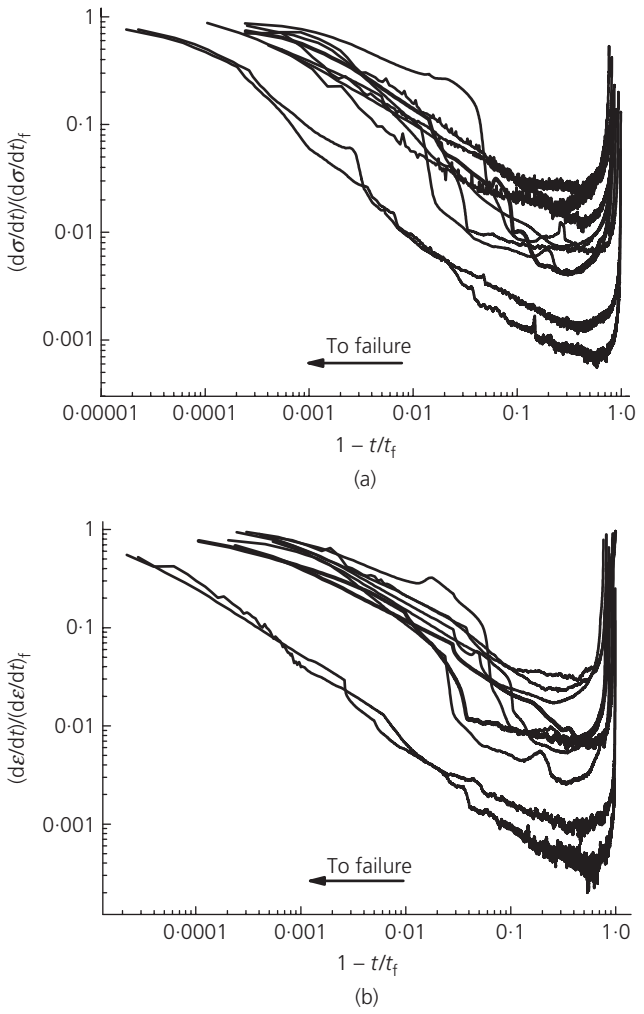

Figure 6. Stress-relaxation and strain rates for all ten specimens. The logarithmic timescale $1 - t/t_f$ indicates the power-law behaviour of the stress and deformation prior to macroscopic failure. (a) Log–log plots of the force rate, $d\sigma/dt$, normalised using the values corresponding to macroscopic failure, $(d\sigma/dt)_f$, against time, $1 - t/t_f$. (b) Log–log curve of the strain rate, $d\varepsilon/dt$, normalised using the values corresponding to macroscopic failure, $(d\varepsilon/dt)_f$, plotted against time, $1 - t/t_f$

phase. Consequently, $t_f - t_0$ is the entire duration of creep relaxation. It was found that the stress-relaxation rates and the creep-strain rates near failure could be described well using the following power laws: stress rate $= A[1 - (t - t_0)/(t_f - t_0)]^{-\alpha}$ and strain rate $= B[1 - (t - t_0)/(t_f - t_0)]^{-\alpha}$. In order to determine the values of the exponent, α, an unweighted least-squares linear regression was performed to fit the data. It is obvious that the fitting of the values of the critical power-law exponent was valid only for conditions close to macroscopic failure. Based on the experimental data (Figures 6(a) and 6(b)), the best fit for the critical exponent α could be obtained within the last 1–3% of the entire deformation range ahead of the failure point, t_f. To illustrate the fitting process in detail, Figure 7 shows the results (see the solid lines) for the stress rates (scatters) near failure for two of the concrete specimens as examples. The experimental data for all ten concrete specimens were fitted. Further, the mean critical exponent as well as the standard error was calculated by taking an unweighted mean. The mean power-law exponent $-\alpha$ was $-0{\cdot}58 \pm 0{\cdot}13$ for the stress rate and $-0{\cdot}56 \pm 0{\cdot}12$ for the strain rate; these are almost equal to the theoretical value of $-1/2$ (Hao *et al.*, 2012).

Dependence of time to failure on secondary stage

The plots in Figure 5 demonstrate that the curves for the stress (see curves in Figure 5(a)) and strain rates (see curves in Figure 5(b)) had long segments with an almost constant slope, as indicated by the horizontal parts of the curves. The steady-state stress-relaxation and creep-strain rates could be calculated

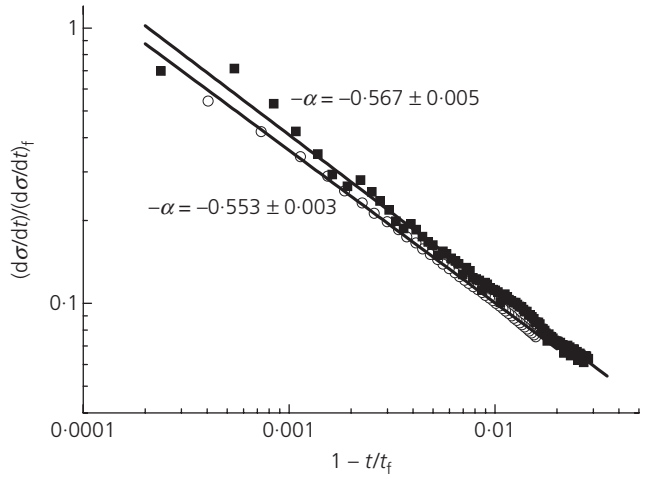

Figure 7. Plots showing the fitting of the power-law expressions (see the solid line) to the experimental data (scatter symbols) for the point near failure for two of the specimens

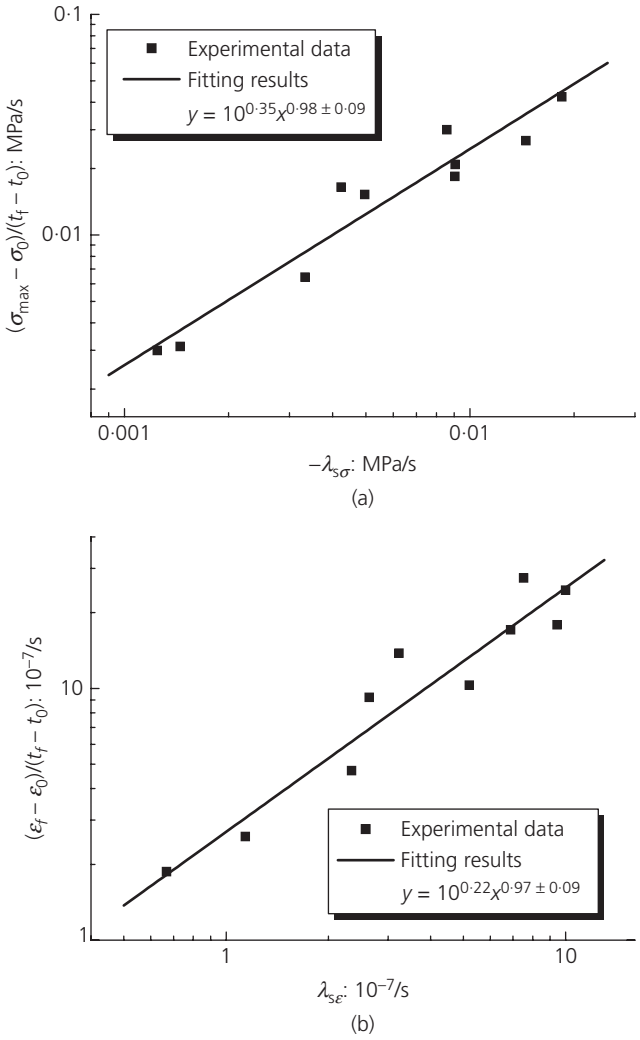

Figure 8. Log–log plots of the creep-relaxation-related slope, λ_s, of the secondary stage and $(\sigma_{max} - \sigma_0)/(t_f - t_0)$, $(\varepsilon_f - \varepsilon_0)/(t_f - t_0)$. It can be seen that there is a power-law relation between the two. The solid straight line is the fitted result. (a) $(\sigma_{max} - \sigma_0)/(t_f - t_0)$ plotted against λ_s and (b) $(\varepsilon_f - \varepsilon_0)/(t_f - t_0)$ plotted against λ_s

for these portions of the creep-relaxation curves. During the brittle creep-relaxation process, the secondary stage dominates the entire lifetime of the concrete specimens. The evolution characteristics during the secondary stage determine the transition from the steady state to the unstable state in the tertiary stage.

During the relaxation process, the energy dissipated is directly proportional to the force, because the energy dissipated is equal to $(FU)/2$ and U is constant. Consequently $\sigma_{max}/(t_f - t_0)$ represents the average rate of energy dissipation during the process of brittle creep relaxation, while the slope, λ_s, corresponding to the secondary relaxation segment, reflects the rate at which energy is consumed in the steady stage. Hence, it can be expected that there exists a relationship between the slope, λ_s, of the segment corresponding to secondary relaxation and $\sigma_{max}/(t_f - t_0)$.

The dependence of the specimen lifetime on the creep slope, λ_s, of the secondary stage is shown in Figure 8. It can be seen that $\sigma_{max}/(t_f - t_0)$ exhibits an almost power-law-like relationship with λ_s; the power-law exponent was $0{\cdot}98 \pm 0{\cdot}09$ for the stress and $0{\cdot}97 \pm 0{\cdot}09$ for the strain. It is clear that, in the case of the present study, a steep creep-related slope in the secondary stage implied a short lifetime. This, in turn, suggested that it may be possible to predict the lifetime of concrete by monitoring the evolution of the secondary stage.

Practical methods for predicting the failure time of concrete

The present results suggest two practical methods for predicting the failure time of concrete. A long-term prediction can be made based on the fact that the increase in the logarithm of the creep-relaxation life, t_f, is proportional to the logarithm of the stress or strain rate, λ_s, in the secondary stage. For stress, this relation can be expressed as follows

$$\sigma_{max}/(t_f - t_0) = 10^{0{\cdot}35}\lambda_s^{0{\cdot}98} \quad (1)$$

Then, the failure time, t_f, can be calculated by measuring the stress rate, λ_s, in the secondary stage. It is interesting that the exponent is 0·98 for the stress and 0·97 for the strain and that both are almost equal to unity, as this will make the predictions easy, because for such cases the failure time has a nearly linear relation with λ_s.

A short-term prediction of failure can be made on the basis of a power law relation in the tertiary stage, namely, on the fact

that the logarithm of the remaining time $(t_f - t)$ decreases in proportion to the logarithm of the rate of strain (or stress). It can be expressed as follows

$$\log v = \log A - \alpha \log (1 - t/t_f) \quad (2)$$

where v represents the rate of an observable quantity, such as strain or stress. Equation 2 contains three unknown parameters: t_f, A and α. Hence, the failure life, t_f, or the remaining life, $(t_f - t)$, at the optional time can be obtained for practical use, if three or more points are properly selected on the creep-relaxation curve.

Shown below is a simplified explanation of the procedure for estimating the time to failure. Choose three successive points (v_1, t_1), (v_2, t_2) and (v_3, t_3) on the tertiary velocity curve, so as to satisfy the following relation

$$\frac{v_2}{v_1} = \frac{v_3}{v_2} \quad (3)$$

Three simultaneous equations are obtained by putting the values of each point in Equation 2. Then, the following relations can be deduced

$$\log \frac{v_2}{v_1} = -\alpha \log \frac{t_f - t_2}{t_f - t_1}. \quad (4)$$

$$\log \frac{v_3}{v_2} = -\alpha \log \frac{t_f - t_3}{t_f - t_2}. \quad (5)$$

Next, Equations 3–5 give

$$\frac{t_f - t_2}{t_f - t_1} = \frac{t_f - t_3}{t_f - t_2}. \quad (6)$$

By rearranging this equation, the failure time can be calculated as follows

$$t_f = \frac{t_2^2 - t_1 t_3}{2t_2 - (t_1 + t_3)}. \quad (7)$$

Conclusions

The experimental results obtained from this study verified that violent brittle failure can be induced in concrete during the process that combines creep and stress relaxation. The rate of decrease of the axial stress was found to increase initially. This was followed by slow relaxation and the subsequent failure of the specimen. These results imply that, in heterogeneous brittle materials such as concrete, the creep-relaxation process may induce macroscopic failure if the elastic energy stored in the surrounding environment can compensate for the fracture energy of the specimen.

In the present study, the load displacement during the creep-relaxation phase was almost equal to the displacement corresponding to the peak stress during the monotonic tests. However, the average maximum stress during the creep-relaxation tests was slightly higher than the average peak stress during the static monotonic tests. In contrast, the strain at maximum stress during the creep-relaxation tests was lower than that during the static monotonic tests. This implies that rapid loading led to the loading apparatus storing a large amount of energy in the initial loading stage during the creep-relaxation tests and that its release is what eventually induced the brittle failure of the concrete samples.

The tested concrete specimens underwent an obvious tertiary stage before macroscopic failure. The strain rate during this tertiary creep-relaxation stage increased rapidly; this was owing to a sharp drop in the stress and eventually resulted in sudden macroscopic failure. The increases in the creep and stress-relaxation rates near failure exhibited power-law behaviours, with the exponents being $-0{\cdot}56 \pm 0{\cdot}12$ for the strain rate and $-0{\cdot}58 \pm 0{\cdot}13$ for the stress rate; these values are approximately equal to the theoretical value of $-1/2$ (Hao *et al.*, 2012).

The curves for the strain and stress rates with respect to time indicated that there exists a long-lasting stage during which the strain and stress rates remain almost constant. This implied that the secondary stage, during which the strain (stress) rate is constant, dominates the lifetime of concrete. A steep slope for the curve for secondary creep relaxation indicates a high λ_s value, which implies a short lifetime. The average creep and stress-relaxation rate, expressed as the total creep strain divided by the lifetime $(t_f - t_0)$, exhibited a power-law dependence on the secondary creep and stress-relaxation rates, with the exponents being $0{\cdot}97 \pm 0{\cdot}09$ for the strain and $0{\cdot}98 \pm 0{\cdot}09$ for the stress. The results of this study suggest that it may be possible to predict the time to failure of concrete by monitoring of its creep-relaxation behaviour in the steady state.

Acknowledgements

This work was supported by the Natural Science Foundation of Hebei province, China (D2015203398), the National Basic Research Program of China (grant no. 2013CB834100), and the Opening Fund of State Key Laboratory of Non-linear Mechanics, Institute of Mechanics, Chinese Academy of Science.

REFERENCES

Aifantis EC and Gerberich WW (1975) A theoretical review of stress relaxation testing. *Materials Science and Engineering* **21(2)**: 107–113.

Aslani F and Maia L (2013) Creep and shrinkage of high-strength self-compacting concrete: experimental and analytical analysis. *Magazine of Concrete Research* **65(17)**: 1044–1058, http://dx.doi.org/10.1680/macr.13.00048.

Barpi F and Valente S (2005) Lifetime evaluation of concrete structures under sustained post-peak loading. *Engineering Fracture Mechanics* **72(16)**: 2427–2443.

Bazant ZP (2001) Prediction of concrete creep and shrinkage: past, present and future. *Nuclear Engineering and Design* **203(1)**: 27–38.

Bazant ZP and Baweja S (1995) Justification and refinements of model B3 for concrete creep and shrinkage 1. Statistics and sensitivity. *Materials and Structures* **28(7)**: 410–415.

Bazant ZP and Pijaudier-Cabot G (1988) Nonlocal continuum damage, localization instability and convergence. *Journal of Applied Mechanics* **55(2)**: 287–293.

Bazant ZP and Xiang Y (1997) Crack growth and lifetime of concrete under long time loading. *Journal of Engineering Mechanics* **123(4)**: 350–358.

Blechman I (2014) Pure creep, maturity and MP-creep in concrete in terms of an exo-process. *Magazine of Concrete Research* **66(10)**: 505–513, http://dx.doi.org/10.1680/macr.12.00065.

Bocca PG and Antonaci P (2005) Experimental study for the evaluation of creep in concrete through thermal measurements. *Cement and Concrete Research* **35(9)**: 1776–1783.

Brooks JJ (2005) 30-year creep and shrinkage of concrete. *Magazine of Concrete Research* **57(9)**: 545–556, http://dx.doi.org/10.1680/macr.2005.57.9.545.

Brooks JJ and Neville AM (1977) A comparison of creep, elasticity and strength of concrete in tension and in compression. *Magazine of Concrete Research* **29(100)**: 131–141, http://dx.doi.org/10.1680/macr.1977.29.100.131.

Carpinteri A, Valente S, Zhou FP, Ferrara G and Melchiorri G (1997) Tensile and flexural creep rupture tests on partially damaged concrete specimens. *Materials and Structures* **30(5)**: 269–276.

Choi H, Lim M, Choi H, Noguchi T and Kitagaki R (2015) Modelling of creep of concrete mixed with expansive additives. *Magazine of Concrete Research* **67(7)**: 335–348, http://dx.doi.org/10.1680/macr.14.00249.

Denarié E, Cécot C and Huet C (2006) Characterization of creep and crack growth interactions in fracture behaviour of concrete. *Cement and Concrete Research* **36(3)**: 571–575.

Forth JP (2015) Predicting the tensile creep of concrete. *Cement and Concrete Composites* **55**: 70–80, http://dx.doi.org/10.1016/j.cemconcomp.2014.07.010.

Gao Y, Zhang J and Han P (2013) Determination of stress relaxation parameters of concrete in tension at early-age. *Construction and Building Materials* **41(2)**: 152–164.

Geng Y, Ranzi G, Wang Y and Zhang S (2012) Time-dependent behaviour of concrete-filled steel tubular columns: analytical and comparative study. *Magazine of Concrete Research* **64(1)**: 55–69, http://dx.doi.org/10.1680/macr.2012.64.1.55.

Hamed E (2015) Non-linear creep effects in concrete under uniaxial compression. *Magazine of Concrete Research* **67(16)**: 876–884, http://dx.doi.org/10.1680/macr.14.00307.

Hao SW, Xia MF, Ke FJ and Bai YL (2010) Evolution of localized damage zone in heterogeneous media. *International Journal of Damage Mechanics* **19(19)**: 787–804.

Hao SW, Zhang BJ and Tian JF (2012) Relaxation creep rupture of heterogeneous material under constant strain. *Physical Review E* **85(1)**: 012501.

Jansen DC and Shah SP (1997) Effect of length on compressive strain softening of concrete. *Journal of Engineering Mechanics* **123(1)**: 25–35.

Klug P and Wittmann F (1970) The correlation between creep deformation and stress relaxation in concrete. *Matériaux et Construction* **3(2)**: 75–80.

Omar M, Loukili A, Pijaudier-Cabot G and Le Pape Y (2009) Creep-damage coupled effects: experimental investigation on bending beams with various sizes. *Journal of Materials in Civil Engineering* **21(2)**: 65–72.

Ranaivomanana N, Multon S and Turatsinze A (2013) Basic creep of concrete under compression, tension and bending. *Construction and Building Materials* **38(1)**: 173–180.

Rossi P, Tailhan JL, Le Maou F, Gaillet L and Martin E (2012) Basic creep behaviour of concretes. Investigation of the physical mechanisms by using acoustic emission. *Cement and Concrete Research* **42(1)**: 61–73.

Rossi P, Boulay C, Tailhan JL, Martin E and Desnoyers D (2014) Macrocrack propagation in concrete specimens under sustained loading: study of the physical mechanisms. *Cement and Concrete Research* **63**: 98–104.

Saliba J, Grondin F, Matallah M, Loukili A and Boussa H (2013) Relevance of a mesoscopic modeling for the coupling between creep and damage in concrete. *Mechanics of Time-Dependent Materials* **17(3)**: 481–499.

Shah SP, Choi S and Jansen DC (1994) Strain softening of concrete in compression. Strain softening of concrete, committee report 148SSC. In *Proceedings of 48th General Council, Technical Session*. Rilem, Trento, Italy, pp. 1827–1841.

Van Mier JGM, Shah SP, Arnaud M *et al.* (1997) Strain-softening of concrete in uniaxial compression. *Materials and Structures* **30(4)**: 195–209.

Voight B (1989) A relation to describe rate-dependent material failure. *Science* **243(4888)**: 200–203.

WHAT DO YOU THINK?

To discuss this paper, please submit up to 500 words to the editor at journals@ice.org.uk. Your contribution will be forwarded to the author(s) for a reply and, if considered appropriate by the editorial panel, will be published as a discussion in a future issue of the journal.